



An island apart: Cranial endocast variation and sensory function in Tenrecomorpha

R. Benjamin Sulser¹ · Ross D. E. MacPhee²

Accepted: 19 April 2023 / Published online: 23 June 2023

© The Author(s), under exclusive licence to Springer Science+Business Media, LLC, part of Springer Nature 2023

Abstract

It has long been recognized that, among extant mammals, the afrotherian clade Tenrecomorpha contains an exceptional range of sensory specialists in which arboreal, fossorial, semiaquatic and possibly even echolocating species occur within a single clade. Despite their obvious interest in this regard, the sensory apparatus of these animals has not been investigated with modern techniques. Presented here is a geometric morphometric analysis of virtual endocasts of 24 tenrecomorph species (~69% of extant diversity) reconstructed via high-resolution uCT techniques. Utilizing linear regression and PCA analyses we identify a model including allometry, habitat, and evolutionary history as the main factors underlying shape variability. Distinct clusters in the tenrecomorph morphospace correspond to shifts within the olfactory and cortical regions of the brain, which covary with independent evolution of aquatic and fossorial behaviors. These results showcase remarkable instances of sensory convergence within the clade and provide a template for inter- and intra-clade analyses of this distinctive branch of the mammal tree.

Keywords Endocast · Evolution · Morphometrics · Tenrecidae

Introduction

The afrotherian mammal clade Tenrecomorpha contains a wide array of distinct sensory ecomorphotypes (Olson 2013; Everson et al. 2016), including arboreal, fossorial, semiaquatic, and even echolocating (Gould 1965) behaviors. These specializations are distributed among ~35 extant, narrowly distributed species, with contemporary phylogenies placing all in suborder Tenrecomorpha (Everson et al. 2016), containing the families Tenrecidae and Potamogalidae, the latter then result of elevating the former subfamily Potamogalinae to family status. Since their arrival on the island of Madagascar between 50–20 Ma (Ali and Huber 2010;

Samonds et al. 2012; Everson et al. 2016), these insectivores have since evolved into a dazzling array of distinct ecological niches. However, the degree to which these adaptations are reflected in tenrecomorph anatomy remains controversial: previous studies on skull morphology (e.g., Finlay and Cooper 2015) have documented surprisingly little disparity within the clade (in large part due to similarities encountered in the most speciose genus, *Microgale*), while those focusing on the postcranial skeleton (Salton and Szalay 2004; Salton and Sargis 2008a, b, 2009) found that cladistic and ecomorphotype signals varied, depending on the specific skeletal components investigated.

Small mammals with similar sensory adaptations exhibit highly specialized internal sensory structures, such as trade-offs between visual and olfactory brain structures in bats and primates (Barton et al. 1995), well-developed trigeminal systems in semiaquatic mammals (Sánchez-Villagra and Asher 2002), and the size of the eyes, ethmoid, and tympanic membrane in various taxa across ecological niches (Nummela et al. 2013). Given the range of sensory adaptations evident in tenrecomorph species and the conflicting signals found in osteological studies, understanding the soft tissue structures underpinning function in ecomorphotypes would be an essential step in recovering not only tenrecomorph evolutionary

✉ R. Benjamin Sulser
rsulser@amnh.org

Ross D. E. MacPhee
macphee@amnh.org

¹ Richard Gilder Graduate School, American Museum of Natural History, Central Park West & 79th St, New York, NY 10024, USA

² Department of Mammalogy, American Museum of Natural History, Central Park West & 79th St, New York, NY 10024, USA

history, but also the nature of convergent evolution of neurosensory structures (Sulser 2022). Should cranial anatomy vary according to ecomorphotype, and correspond to neuroanatomical trends identified in other groups (e.g., olfactory bulb reduction in aquatic mammals; Sánchez-Villagra and Asher 2002), then tenrecs would be expected to exhibit anatomical convergence with phylogenetically distant groups for such features and may utilize similar genomic and developmental pathways to produce these sensory specializations. Similarly, if signals of novel variation (or no signal at all) are recovered, then tenrecs might represent an exception to conclusions based on studies of brain shape determined primarily from non-afrotherian mammals, suggesting potential broad-scale clade distinctions within mammals.

Cranial endocasts represent an oft-utilized metric for the representation of brain shape (Watanabe et al. 2018; Dumoncel et al. 2021). While endocasts may not capture all aspects of neuroanatomical variation, particularly with respect to neural density and size, as in the case of cortical regions (Collins et al. 2010; Herculano-Houzel et al. 2015), they are nonetheless useful for evaluating sensory evolution in small mammals both extant (Ahrens 2014; Bertrand et al. 2019) and extinct (Silcox et al. 2010; Bertrand et al. 2018; Ni et al. 2019). Thus, anatomical description and intraclade comparison of tenrecomorph cranial endocasts may be helpful in shedding light on areas of potential functional relevance. Hereafter, the term “endocast” should be assumed to refer to volumetric representations of the interior of the brain case exclusively.

In this study, we investigate virtual endocasts collected from 24 taxa across Tenrecomorpha (Potamogalidae + Tenrecidae). We anatomically characterize each major subfamily, and use landmark-based geometric morphometrics (GM) (Zelditch et al. 2012), phylogenetic least-squares regression (PGLS) (Adams 2014a) and principal component analysis (PCA) to understand the nature of endocast variation within the tenrecomorph sensory system. We explicitly test the hypothesis that tenrecomorph sensory anatomy, as reflected in endocast shape, varies across and in correlation with sensory ecomorphotype.

Materials and methods

Specimens for this project were loaned from the mammalogy collections of the American Museum of Natural History (AMNH) and The Field Museum (FMNH) (see Table 1). All were scanned on the GE Phoenix Vtome x SMicroCT scanner housed in the AMNH Microscopy and Imaging Facility (MIF). Scans were performed with resolutions of 18–56 μm . Image stacks were generated and endocasts reconstructed utilizing Mimics software (Materialise Mimics 2020). Endocasts were segmented via a combination of Multiple Slice

Table 1 Taxon names and numbers used in this study

Taxon name	Specimen number	Reference in PCA
<i>Echinops telfairi</i>	AMNH 170599	1
<i>Geogale aurita</i>	FMNH 173143	2
<i>Hemicentetes semispinosus</i>	AMNH 275193	3
<i>Microgale brevicaudata</i>	AMNH 275743	4
<i>Microgale cowani</i>	AMNH 275000	5
<i>Microgale drouhardi</i>	AMNH 275088	6
<i>Microgale fotsifotsy</i>	AMNH 275130	7
<i>Microgale gymnorhyncha</i>	AMNH 275134	8
<i>Microgale jobihely</i>	AMNH 274982	9
<i>Microgale longicaudata</i>	AMNH 275141	10
<i>Microgale mergulus</i>	AMNH 100689	11
<i>Microgale parvula</i>	AMNH 275155	12
<i>Microgale soricoides</i>	AMNH 275172	13
<i>Microgale taiva</i>	AMNH 275018	14
<i>Microgale thomasi</i>	AMNH 275355	15
<i>Micropotamogale lamottei</i>	FMNH 162893	16
<i>Micropotamogale ruwenzorii</i>	FMNH 207665	17
<i>Nesogale dobsoni</i>	AMNH 275033	18
<i>Nesogale talazaci</i>	AMNH 207003	19
<i>Oryzorictes hova</i>	AMNH 275189	20
<i>Oryzorictes tetradactylus</i>	AMNH 31243	21
<i>Potamogale velox</i>	AMNH 51334	22
<i>Setifer setosus</i>	AMNH 170535	23
<i>Tenrec ecaudatus</i>	AMNH 170523	24

Edit and Threshold functions to select the “empty space”, i.e., volumes less dense than bone within the cranial cavity. The resulting segmented endocranial models were pruned by hand to ensure a solid continuous mesh prior to export for landmark collection. Three-dimensional landmarks were placed along the left and midline of the skull using Landmark Editor 2.7 (Wiley 2005) (Fig. 1, Table 2). All bilaterally symmetrical points were mirrored prior to general Procrustes analysis (GPA), as side-only landmark studies are known to contain errors (Cardini 2017). Landmarks were chosen based on their repeatability and relevance for outlining the margins of major brain regions (Ahrens 2014; Bertrand et al. 2018, 2019).

Morphometric analyses were performed in R (R Core Team 2013), utilizing the packages Geomorph (Adams and Otárola-Castillo 2013), RGL, and Paleomorph. General Procrustes analysis (GPA) (Zelditch et al. 2012) was performed in order to orient and scale all specimens prior to downstream analyses. In order to identify evolutionary signal, the K-statistic (Adams 2014b) was estimated from the full dataset utilizing *physignal* and a published phylogenetic tree (Everson et al. 2016). Procrustes ANOVA and PGLS (Adams and Collyer 2018) tests were run using the *ProcD*.

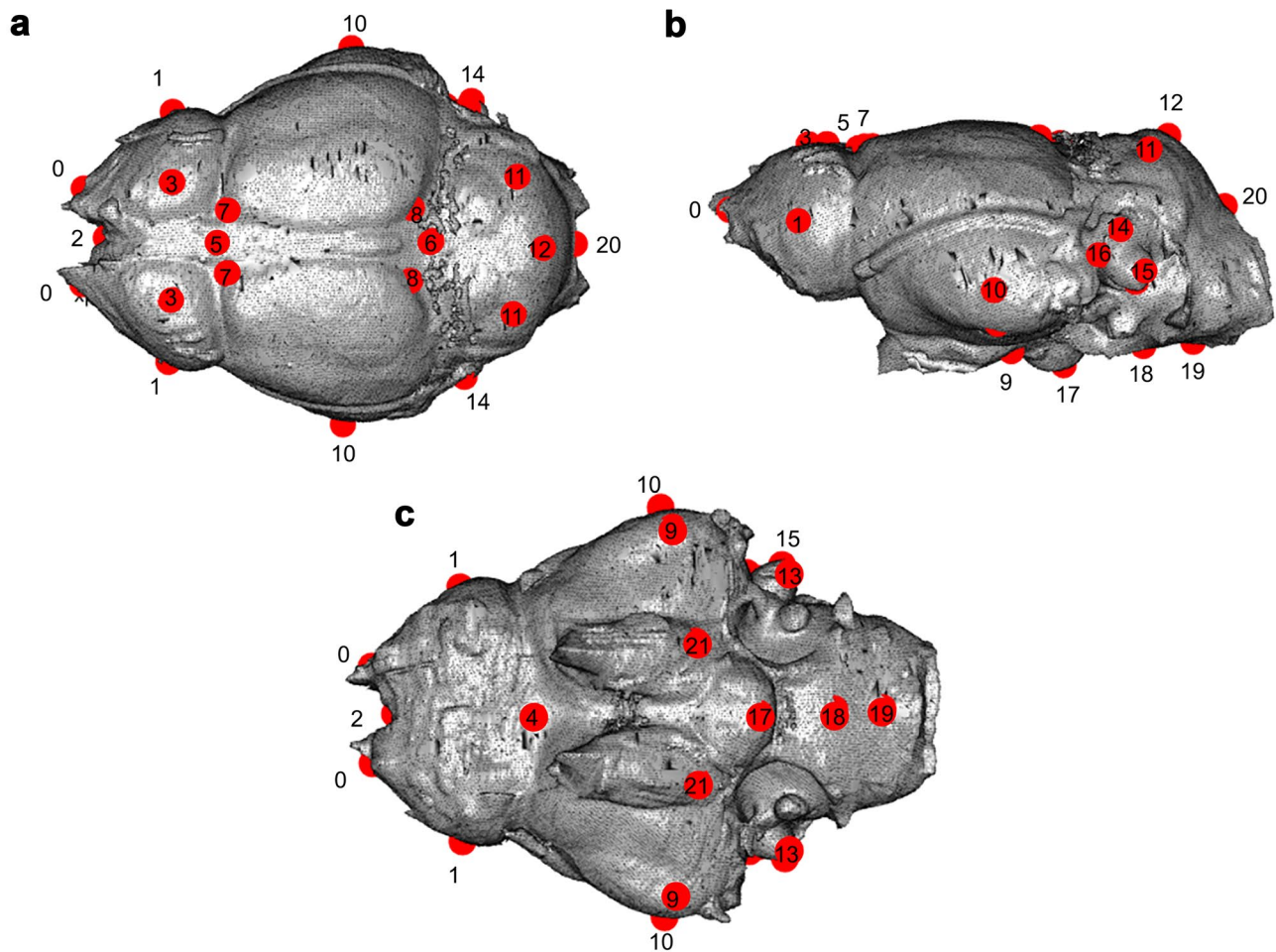


Fig. 1 Illustration of landmarks utilized in this analysis in three views: dorsal (a), lateral (b), and ventral (c). Landmark numbers are listed, with bilateral landmarks listed on each side noted to correspond with Table 2

Lm, *ProcD.pgl*s and *anova* functions to explore the relationships between different potential covarying factors according to published literature (diet, ecomorphotype, habitat, and locomotion), in addition to the potential effects of allometry (as observed through log centroid size). A list of all factors analyzed and citations for each can be found in Online Resource 1. All permutations of PCA were performed utilizing *gm.prcomp* (Collyer and Adams 2021).

Results

After Procrustes alignment and ordination, testing via the K-statistic confirms the presence of significant evolutionary signal in the dataset (observed $K = 0.681$, $P < 0.001$, Fig. 2). The results of ANOVA regression and PGLS are available in Online Resource 2. In single-factor ANOVA analyses, ecomorphotype and diet explain the most variation, while in single-factor PGLS testing

habitat was the sole statistically significant factor. When multiple factors are taken into account, a regression model including both ecomorphology and habitat was found to be the best fit (R-squared value $\sim 43\%$, $P > 0.001$ under ANOVA; R-squared value $\sim 30\%$, $P > 0.002$ under PGLS; see Online Resource 2). Given the highly variable per-taxon sample sizes in this study (e.g., few examples of semiaquatic Potamogalidae vs. abundant and overlapping examples of speciose terrestrial insectivores within *Microgale*) means that PGLS results should be viewed with caution.

PCA results are shown in Figs. 3, 4, and 5. To better quantify shape variation attributed to phylogeny, the shape space was run under a GLS rotation (Collyer and Adams 2021) to visualize shape variation with minimal phylogenetic influence (Fig. 4). Phylogenetically aligned component analysis (PaCA) was also run, and results are available in Online Resource 3.

Table 2 Type 1 landmarks utilized in this study

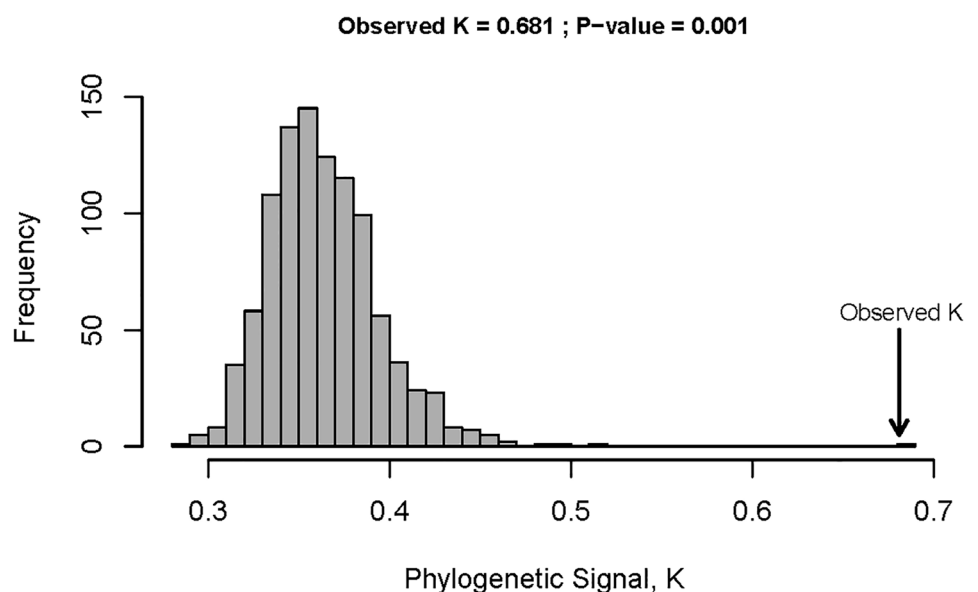
Point	Locale	Bilateral or midline
0	Rostral (anterior) terminus of olfactory bulb	Bilateral
1	Lateral terminus of olfactory bulb	Bilateral
2	Center-anterior end of olfactory bulb	Midline
3	Superior-most point on olfactory bulb	Bilateral
4	Inferior fossa of olfactory bulb	Midline
5	Confluence of circular and sagittal fissures	Midline
6	Confluence of sinuses (pyramid)	Midline
7	Neocortex- Rostral terminus	Bilateral
8	Neocortex—Posterior terminus/Corner formed by confluence of sinuses	Bilateral
9	Ventral-most point on piriform lobe	Bilateral
10	Lateral-most point on piriform lobe	Bilateral
11	Highest caudal point of occipital pole	Bilateral
12	Vermis	Midline
13	Ventral-most point on petrosal lobule	Bilateral
14	Dorsal-most point on petrosal lobule	Bilateral
15	Lateral-most point on petrosal lobule	Bilateral
16	Rostral-most point on petrosal lobule	Bilateral
17	Hypophyseal fossa	Midline
18	Dorsum sellae	Midline
19	Endobasion	Midline
20	Endopisthion	Midline
21	Foramen ovale exit	Bilateral

With respect to the groupings in the unadjusted PCA, the first component accounted for 31.75% of the variation in the dataset, with the second and third representing 15.44% and 11.11%, respectively (all other components each accounted

for <9% of the total variance) (Fig. 3). The sample mesh for the positive PC1 values reflects a quite compressed and rounded endocast, a markedly “pinched” hindbrain (neocortex higher than any lobe on the cerebellum). The piriform lobes are compressed mediolaterally yet expanded ventrally, whilst the negative extreme in PC1 presents anteroposterior elongation of the entire endocast in the morphospace. There is also a relatively long pons, medulla, and cerebellum with relatively small paraflocculi, as well as an expanded olfactory region. With respect to PC2, the positive axis represents large olfactory bulbs and mediolaterally expanded piriform lobes, all larger than the brainstem; the negative values represent exceptionally small olfactory bulbs, a drastically reduced anterior piriform cortex with an expanded neocortex (creating a sloped effect anteriorly), a widened hindbrain larger in mediolateral width than the olfactory bulbs, and a dorsoventrally compressed cerebellar region. The PC2 negative values also show that the exit apertures of the oval foramina for the mandibular nerve are closer together than on the positive axis and are compressed mediolaterally. Finally, the PC3 positive axis represents a smooth neocortex that is higher than any point on the cerebellum, with a dorsal expansion and mediolateral compression of the neocortex and piriform cortex. By contrast, the negative axis represents a marked “pinching” at the anterior margin of the cortices near the olfactory bulbs, with a corresponding mediolaterally expanded cerebellum that also exhibits a vermis higher than the neocortex.

Several patterns can be identified via the groups present within these first three PCA components. All semiaquatic taxa (*Potamogale*, *Micropotamogale*, and *Microgale mer-gulus*, yellow) group with one another, near the negative extreme of PC2, whilst arid-adapted tenrecines occupy a

Fig. 2 K-statistic output from *physignal* (Adams and Otárola-Castillo 2013) indicating the significance and magnitude of evolutionary signal. $K < 1$ (indicated by the arrow), suggesting that closely-related taxa in this analysis exhibit a higher degree of common variance than would be expected under a Brownian model of evolution. See Adams (2014b) for more details



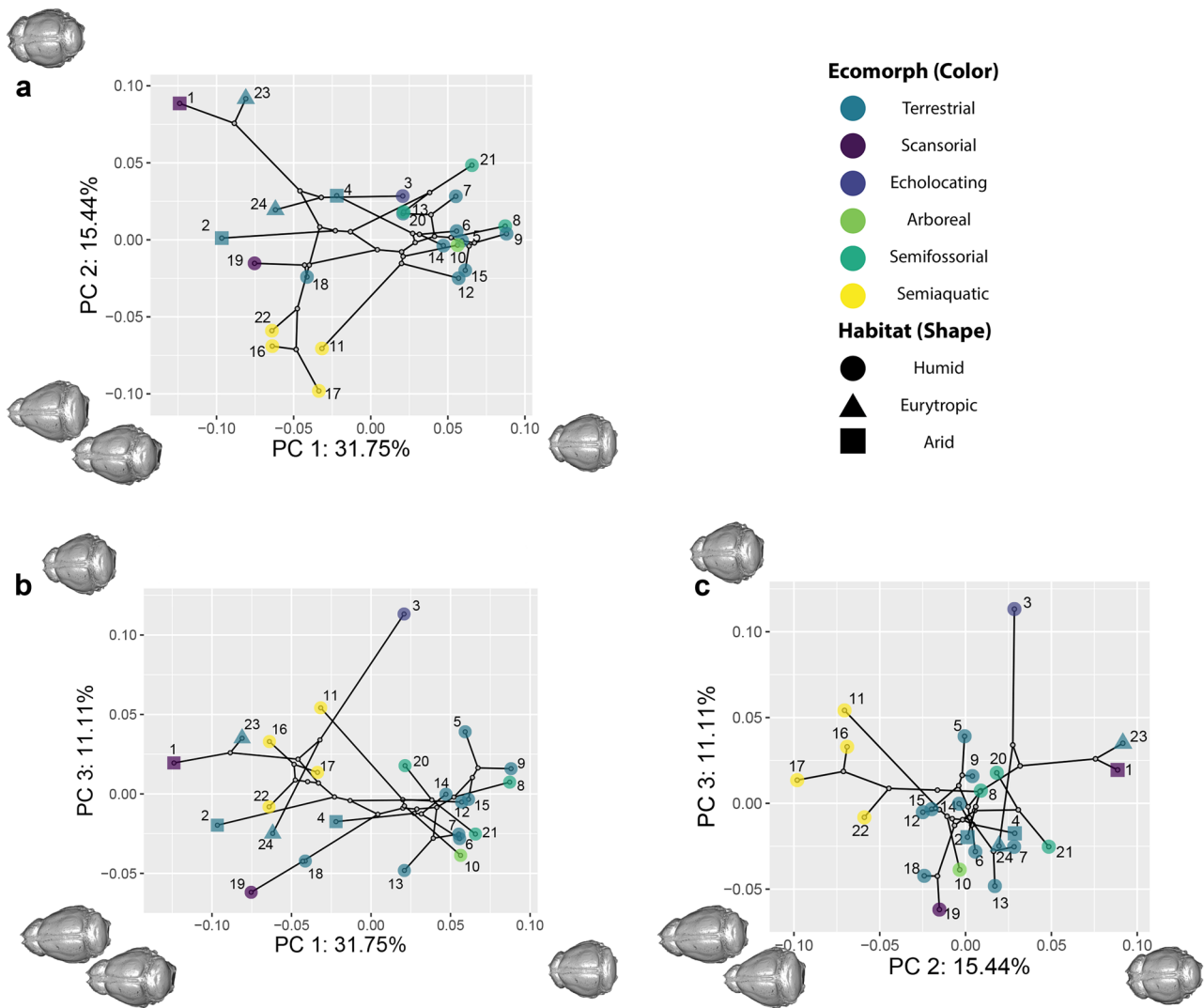


Fig. 3 Morphospace results from the first three components of PCAs on all endocasts used in this study. Components 1 (**a** and **b**), 2 (**a** and **c**), and 3 (**b** and **c**) are visualized. All other components account for less than 10% of the total variation. Taxa are characterized by color (indicating ecomorphotype) and shape (indicating habitat). To aid in visualizing the representative shapes, sample meshes have been cre-

ated from the extreme of each positive and negative value for each axis using the function *warpRefMesh* in the *Geomorph* package (Adams and Otárola-Castillo 2013) for each component. Each mesh is plotted in the dorsal view using *Echinops telfairi* as a template. The phylogenetic tree connecting each taxon is adapted from Everson et al. (2016). Taxa referred to by each data point can be found in Table 1

distinct region of the morphospace. The sole exception to this generalization, *Hemicentetes semispinosus*, occurs in mesic lowland habitats. Nearly all oryzorictines form a cluster with *Hemicentetes*, with three exceptions: *Microgale mergulus* and the two species of *Nesogale*. Comparison between PC1 and PC3 highlights the disparity found in the tenrecines (*Hemicentetes* in particular) and marks the distinctiveness of *Nesogale* in comparison to species of *Microgale*, which is in line with skeletal (Thomas 1918) and genetic (Everson et al. 2016) arguments for distinguishing these genera. In contrast, comparing PC2 with PC3 compresses all oryzorictines and *Geogale* into the center of the morphospace but highlights the degree to which *Microgale mergulus* uniquely clusters

with the potamogalids and further underlines the separation of *Hemicentetes* from the rest of the Tenrecomorpha.

Remarkably, the PaCA morphospace (Online Resource 3) for these data neatly reinforces the findings in the unadjusted PCA, suggesting these first two principal components are related to evolutionary history and phylogeny. The minima and maxima for the first axis in both the PaCA and PCA analyses resolve similar brain shapes and, while the second axis flips the shapes assigned to minimum and maximum, the resulting phylomorphospaces are otherwise nearly identical. It is perhaps expected, then, that removing the phylogenetic signal (either utilizing transformed or untransformed projections; Collyer and Adams 2021) (Fig. 4c-d) collapses several

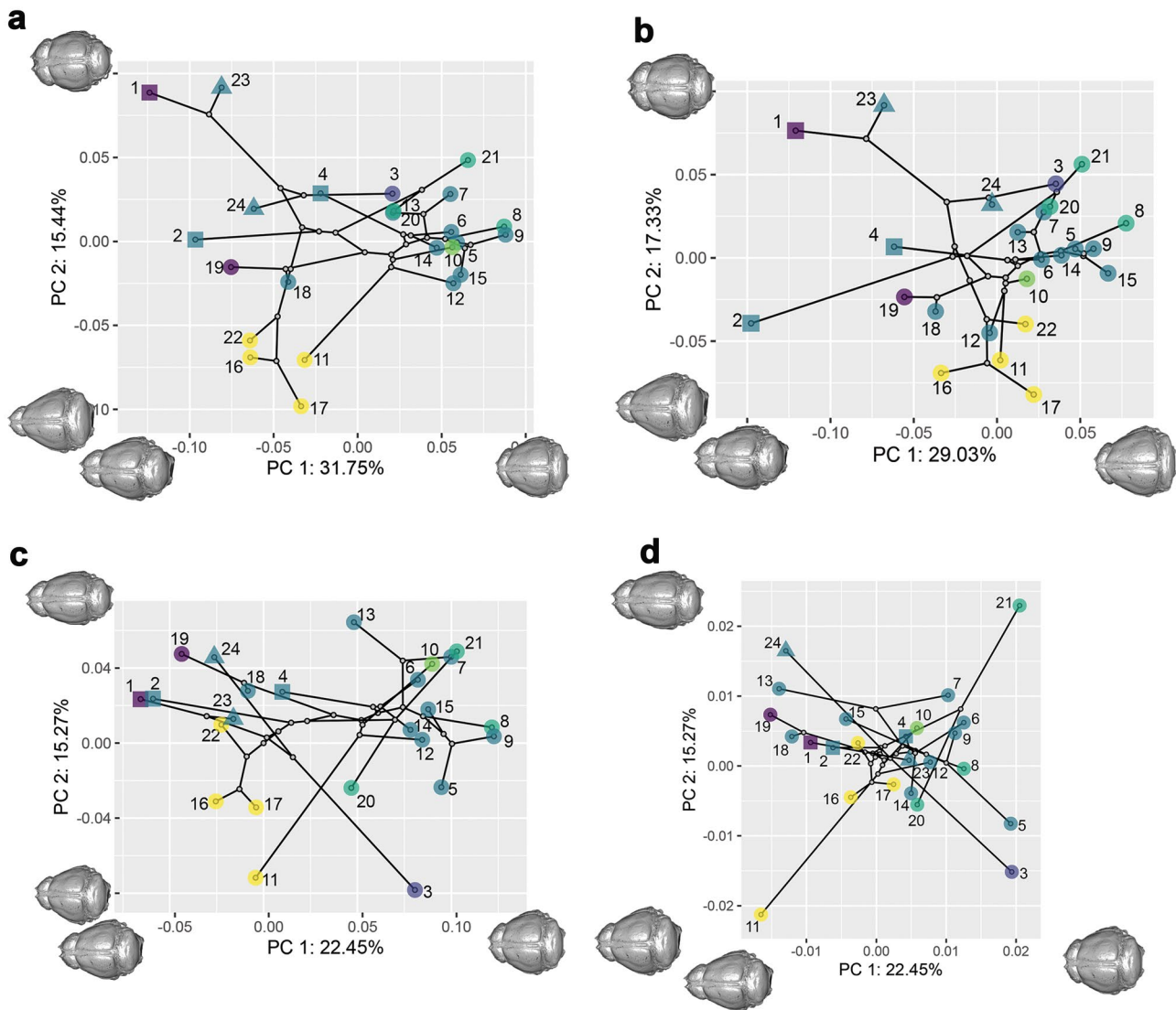


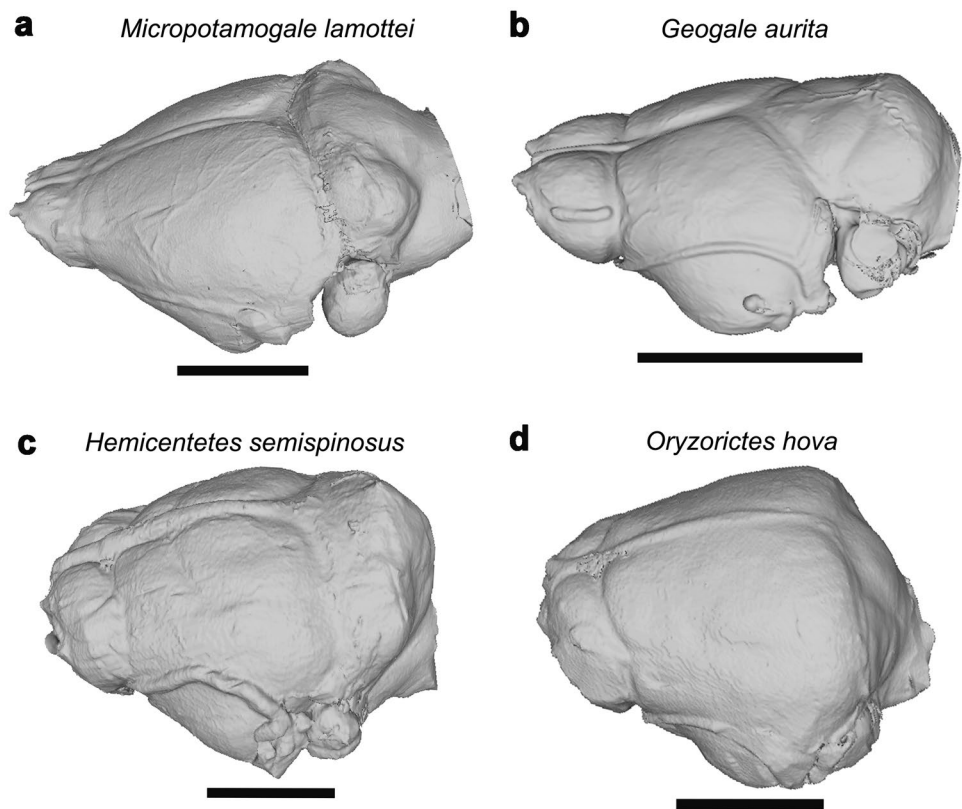
Fig. 4 Morphospace results from the first two components of principal component analyses on all cranial endocasts used in this study under a variety of transformations with respect to phylogenetic covariance: **a.** standard PCA (identical to Figs. 2 and 3a); **b.** PCA after allometric adjustment (see Materials and methods); **c.** phylogenetic PCA (untransformed); and **d.** phylogenetic PCA (with transformed projection of residuals). Taxa are characterized by color (indicating ecomorphotype) and shape (indicating habitat); see Fig. 3 for legend.

of these components, with the PCA transformed projection clustering most taxa in the center of the morphospace. In this transformed morphospace, the first principal component is virtually unchanged, whereas the negative and positive axes of the second component of the transformed PCA portrays a minimum with a lengthened hindbrain and wider, flaring piriform lobes compared to a maximum value with smaller piriform lobes and a sloping neocortex – all of which yields a result remarkably similar to those produced in principal component 3 of the untransformed PCA.

To aid in visualizing the representative shapes, sample meshes have been created from the extreme of each positive and negative value for each axis using the function *warpRefMesh* in the *Geomorph* package (Adams and Otárola-Castillo 2013) for each component. Each mesh is plotted in dorsal view using *Echinops telfairi* as a template. The phylogenetic tree connecting each taxon is adapted from Everson et al. (2016). Taxa referred to by each data point can be found in Table 1

Allometry was found to be statistically significant in our analyses of shape (R-squared value $\sim 30\%$, $P < 0.0004$; Online Resource 2), and for this reason, the potential effects of size on the shape analyses recovered were also investigated. To account for allometry, all PCA plots were replicated on the residuals of a regression of shape against log centroid size (Fig. 4b, Online Resource S3). Minimizing the allometric component from these analyses drastically shifts the morphospace, as might be expected from the statistically significant relationship between size and shape recovered

Fig. 5 Endocast renderings of individual tenrec species for comparison. **a.** *Micropotamogale lamottei* (Potamogalidae); **b.** *Geogale aurita* (Geogalinae); **c.** *Hemicentetes semispinosus* (Tenrecinae); and **d.** *Oryzorictes hova* (Oryzorictinae). Scale bars equal 5 mm. For additional views and renderings, see 3D PDFs in Online Resources 4–7



from ANOVA testing. When adjusted for this component, the semifossorial species in the genus *Oryzorictes* and *Microgale gymnorhyncha* cluster together with *Hemicentetes semispinosus*, while the Potamogalidae + *M. mergulus* cluster expands in morphospace occupation, with borders near the terrestrial and arboreal species of *Microgale*. Of particular note is the fact that the monotypic member of subfamily Geogalinae (*Geogale aurita*) occupies the minimum of both principal axes. On the whole, the adjusted component analysis (Fig. 4b) still reflects the phylogenetic and ecological signals observed in the other PCA, including a distinct region for arid-adapted tenrecines, tight clustering of the oryzorictines, and separate groupings among the semiaquatic taxa. Transforming the dataset to remove phylogenetic signal, however, results in an amorphous “cluster” of taxa with no clear groupings (Online Resource 3), a sign that no strong ecological signal occurs once the factors of phylogeny and allometry have been removed.

Cranial endocast renditions of representative samples for each clade analyzed are presented in Figs. 1 and 5, and Online Resources 4–7. Members of the clade Potamogalidae, represented here by *Micropotamogale lamottei* (Fig. 5a), exhibit drastically reduced olfactory bulbs and olfactory tubercles, albeit with an expanded neocortex and a flattened cerebellum with a distinctive “arrowhead” shape. By contrast, the sole species in the clade Geogalinae, *Geogale aurita* (Fig. 5b), displays extended and enlarged olfactory

regions, which are angled and raised above the level of the cortices in lateral view. In keeping with the study by Stephan et al. (1991), the neocortex appears particularly reduced, but areas of the endocast corresponding to the piriform lobe are relatively robust. The cerebellum appears dorsoventrally flattened, with no rounded “pinching” or mediolateral extension noted in other similar-sized tenrecs. Clade Tenrecinae, exemplified by *Echinops telfairi* (Fig. 1) displays relatively large olfactory bulbs alongside reduced cortices and hind-brain. *Hemicentetes semispinosus* (Fig. 5c) is an exception within this clade, presenting instead relatively small olfactory bulbs and a bulging cerebellum. Finally, *Oryzorictes hova* is marked by relatively large olfactory bulbs, a “rounded” brain (including a flattened cerebellum with a vermis below the neocortex), and an extended piriform lobe that dips below the bottom of the endocast (Fig. 5d).

Discussion

When comparing the effects of size, shape, and ecomorphotype on the form of tenrecomorph endocasts, the influence of ecomorphotype is clearly evident. But it also is clear that evolutionary signal, allometry, and habitat all play a statistically significant role in shaping the tenrecomorph endocast, as supported by *Kmult* and ANOVA testing (see Online Resource 2). Furthermore, ANOVA tests and the

results of morphospace adjustment indicate that these factors are not independent. Given that discernable clustering vanishes within the morphospace when evolutionary history and allometry are removed from the analysis, it is likely that these two factors are dominant in their effect on tenrecid endocranial variation. Ecomorphology and habitat certainly help explain the groupings observed in this analysis (and are statistically significant in the Procrustes ANOVA results) but may only provide a weak signal when assessed separately from evolutionary history and allometry as primary influences on clustering in endocast morphospace. The first principal component in the unaltered analysis, in particular, appears to be highly correlated with allometry. Within this sample, larger taxa show a lengthening of the olfactory bulbs and a pronounced vermis while smaller taxa exhibit wide petrosal lobule regions and a distinct “rounding” of the entire endocast (dorso-ventral expansion and rostral compression, with a short brainstem and flattened olfactory bulbs). Not all subfamilies display an equal amount of variation. Indeed, in keeping with previous morphometric analyses (Finlay and Cooper 2015), the genus *Microgale* is found to be relatively constrained morphologically, with the notable exception of *M. mergulus*. The tenrecines are responsible for driving an unexpectedly large amount of the variation observed across the entire tenrecid morphospace, even after accounting for allometry. The semiaquatic morphotype appears especially distinctive, as potamogalids and *M. mergulus* cluster together in nearly all analyses, even though they are widely separated phylogenetically. In agreement with the high degree of evolutionary signal observed, each subfamily has unique aspects with respect to their distribution within morphospace, as we now summarize.

Potamogalidae

Several studies (Sánchez-Villagra and Asher 2002; Salton and Sargis 2008b, 2009) have noted the effect of semiaquatic adaptations on morphology in this clade, influencing the foramen magnum, infraorbital foramen, the acetabulofemoral joint, and aspects of the pisiform. In this regard, the endocast proves no exception. Semiaquatic tenrecomorph taxa cluster near the higher end of PC2 in the unadjusted morphospace, in agreement with previous studies investigating the semiaquatic ecomorphotype of small mammals. In particular, reduced olfactory regions are consistent with other semiaquatic adaptations in the clade (Stephan et al. 1991). Reduced olfactory capabilities represent a trade-off in sensory specializations (perhaps in favor of somatosensation) in potamogalids, and their large hindbrain and brainstem may reflect an increased demand for fine motor control in navigating an aquatic environment. This clade is not immune to allometric adjustment, as removing the allometric component from this analysis

(Fig. 5) expands the originally tightly clustered group to cover more of the remaining morphospace. This is perhaps not unexpected, as one might expect evolutionary and ecological factors to drive variation once the relationship between size and shape is removed. It is also worth noting that semiaquatic species cluster with *Microgale mergulus* unless evolutionary history is transformed out of the analysis. This should not be taken to imply that *M. mergulus* is closely related to this clade, but rather that the derived anatomical variation within the Potamogalidae is correlated with the semiaquatic ecomorphotype, and thus shows exceptional inter-family convergence between two widely separated branches of the Tenrecomorpha.

Tenrecidae: Geogalinae

The sole member of the subfamily Geogalinae, *Geogale aurita*, has previously been placed ancestral to the other tenrec clades (Olson and Goodman 2003), and for this reason has been interpreted as exhibiting markedly conservative brain characters (e.g., Stephan et al. 1991). Despite its diminutive size, *G. aurita* occupies a distinct region of the unadjusted morphospace along the minimum extreme of PC1 and exhibits on the whole a far more elongate endocast than the comparably sized oryzorictines. These features are clearly distinct from other smaller tenrecs, and indeed, when adjusting for allometry (Fig. 4b) *G. aurita* occupies an even more isolated region of the morphospace, robust to phylogenetic correction. While comparatively little is known about the hunting ecology of this animal outside of an apparent propensity for termites (Stephenson and Racey 1993), the piriform lobe and expanded olfactory regions suggest a strong reliance on olfaction in this clade. Despite a small overall size and likely similar ecology, this tenrec stands in contrast to the oryzorictines (see below) in having an elongate and clearly differentiated endocast compared to the flattened, rounded one characteristic of the latter clade (particularly members of the genus *Microgale*).

Tenrecidae: Tenrecinae

The Tenrecinae display remarkable disparity across the endocast morphospace. Interspecies differences are certainly emphasized by allometry, *Tenrec* being the largest extant tenrecomorph (Nicoll 2003), but persist even when the allometric signal is removed from the dataset. Morphospace spread among tenrecines may be explained in part by habitat, as *Hemicentetes* is found in mesic habitats, while all others are xeric or eurytopic (see Online Resource 1). It should be noted that the tenrecines have evolved spines, and it has been previously suggested that this clade evolved both spinescence and reduced brain size in tandem with moving into open habitats (Stankowich and Stensrud 2019). Endocasts of

Setifer and *Echinops*, the hedgehog tenrecs, cluster near each other under nearly all permutations (Fig. 4) a distinct change in shape that corresponds to the overall shrinkage in encephalization quotient (see Stankowich and Stensrud 2019). *Hemicentetes semispinosus*, by contrast, is positioned within the oryzorictine group in the morphospace. Its broad hindbrain sets *H. semispinosus* apart from the rest of the tenrecs in this analysis, highlighted in PC3 of the unaltered analysis. This may be related to its unique ecology, specializing on earthworms (Eisenberg and Gould 1969), utilizing a unique stridulating organ (Endo et al. 2010), and perhaps even echolocating (Gould 1965). The proximity of *Hemicentetes* to the fossorial *Oryzorictes* in the first principal component of all analyses (Figs. 3 and 4) could be explained in part by convergence in ecomorphotypes, as foraging through sound or vibrissae may lead to a reduction in the presumably ancestrally large olfactory bulbs and flattened cortex seen in all other tenrecines. Although not all fossorial mammals converge on the same brain shape (Stephan et al. 1991), reduced cortices and flattened skulls are consistent with this trend (Bertrand et al. 2018).

In contrast to these relatively extreme examples among tenrecine species, the genus *Tenrec* occupies a central region of the morphospace, varying from its nearest relative, *Hemicentetes*, principally along PC1 (corresponding to larger, more defined olfactory bulbs, smaller petrosal lobules, and a flattened cerebellum). While a remarkably generalist taxon with respect to diet and habitat, *Tenrec* is known to use scent for investigation and communication (Eisenberg and Gould 1969), and the olfactory acuity indicated by its endocast may play a role in facilitating these behaviors.

Tenrecidae: Oryzorictinae

The most speciose clade in this analysis, Oryzorictinae, is marked by broadly similar endocast shape, comparatively anteroposteriorly short endocast (with a rounded neocortex, piriform lobes that dip below the base of the endocast), and comparatively large flocculi and paraflocculi in all species in this subfamily. This general pattern is robust to allometric and phylogenetic corrections, but there are exceptions. *Microgale mergulus* consistently groups convergently with less closely related but similarly semiaquatic taxa. *Nesogale* species are distinct from all other tenrecs in the unadjusted analyses, but this may be in large part due to allometry. Once allometry is accounted for, these species group within the *Microgale* cluster, echoing their traditional classification as members of this genus (MacPhee 1987). Perhaps more intriguing is the lack of ecological distinctiveness among these tenrecs: apart from the convergence of *M. mergulus* on other semiaquatic taxa, the arboreal, xeric, and fossorial members of *Microgale* do not form divergent groupings with taxa outside this clade. Some of this may be due to shared

allometric effects – indeed, after allometric adjustment, the fossorial *Oryzorictes* and *M. gymnorhyncha* pull away from the cluster grouping to a distinct morphospace region. The lack of an exceptional fossorial signal in the endocast is in keeping with findings on fossorial insectivorous boreoeutherians (Stephan et al. 1991), as fossorial mammals may forage through smell, somatosensation, echolocation, or any combination of the three. In the case of these taxa, it may be foraging through smell that is paramount, given the extended olfactory regions of the brain. For the prehensile-tailed arboreal tenrecid *M. longicaudata*, the lack of an exceptional endocast shape is something of a puzzle – perhaps the signifiers of ecological signal are better expressed in secondary sensory structures such as the semicircular canals, or the diminutive size of the animal allows for a less-extreme mode of arboreality than a prehensile tail might imply.

Ancestral endocast shape for tenrecs

The ancestral node for the common ancestor of the Tenrecidae is reflected in the mean of the unadjusted dataset (Fig. 3), which stands not only outside the *Microgale* cluster but also quite apart from any clearly defined ecomorphological grouping. The ancestral node for the potamogalids, on the other hand, lies within the morphospace region occupied by semiaquatic taxa with a corresponding reduction in olfactory size and paleocortex, indicating the strong role this ecomorphotype may have played in the history of extant tenrecomorphs on the African continent. Similarly, the history of the Oryzorictinae appears to show allometric shrinkage with each node approaching *Microgale*, while the ancestral node for the tenrecines represents a midpoint between extremes of this clade's shape disparity and not, as some have claimed, proximity to *Geogale*.

In the absence of relevant fossil data, these findings remain tentative and imprecise, as they are based only on the specimens available for this study. Apart from a few late Quaternary taxa (e.g., MacPhee 1986) that differ little from their close relatives, the nature of the fossil record for Malagasy tenrecomorphs was largely ignored until Buckley (2013) proposed on paleoproteomic grounds that the enigmatic genus *Plesiorycteropus* might be a member of this group. Osteological morphology provides little support for this hypothesis or its traditional alternative that, among extant afrotheres, *Plesiorycteropus* is most closely related to *Orycteropus* (for various evaluations of the evidence see MacPhee 1994; Sanchez-Villagra et al. 2007; Tabuce et al. 2008). Although this taxon was not included in the present analysis, limited endocast evidence (Thewissen 1985) indicates that, as compared to *Orycteropus*, *Plesiorycteropus* exhibits a vermis higher than the neocortex and shortened olfactory bulbs. These features are consistent with the projected morphospace region occupied by tenrecines in this study and, interestingly, bear some

anatomical similarities to the extremes of PC3 seen in *H. semispinosus*. Speculatively, the high vermis and shortened olfactory bulbs could be interpreted as traits ancestrally common to tenrecines prior to the evolution of spinescence and related xeric adaptations, but this obviously needs closer study. Alternatively, ontogenetic studies on the cranial endocast of the capybara (Ferreira et al. 2022) suggest that that a comparative lengthening of the olfactory bulbs and a flattening of the vermis occur during ontogenetic growth. It may thus be possible that the divergence observed in *H. semispinosus* could be the result of paedomorphism within this tenrecine branch. In any case, further testing of the possible inclusion of *Plesiorycteropus* within tenrecs is highly warranted.

Comparisons to other mammalian clades

It should be noted that, despite their considerable diversity, the vast majority of tenrecomorph disparity is located on the island of Madagascar. The radiation of Malagasy tenrecs possibly took place in a competitive vacuum; there are no other similarly insectivorous mammals on the island apart from two species of the Neogene soricid *Suncus* (one introduced) (Stephenson et al. 2003). By contrast, apart from a few highly incomplete Miocene fossils (Butler and Hopwood 1957; Asher et al. 2006), the semiaquatic Potamogalidae are the only members of the clade on the African mainland, while multiple species of terrestrial insectivores of different mammalian clades (especially the soricid *Crocidura*) are present in the form of ecotypes (Stephenson et al. 2003). In the absence of a substantial Paleogene fossil record for mainland Africa, the actual factors behind the lack of extant African terrestrial tenrecs, and the role competition (or lack thereof) may have played in the divergent evolutionary paths of each lineage, can only be surmised.

In addition to intra-clade disparity, a growing body of mammalian endocast research permits comparison to other clades of mammals investigated with similar techniques. Strong phylogenetic groupings and a slight degree of fossorial homoplasy can be detected in squirrels and their allies (Bertrand et al. 2019), a situation reminiscent of the tenrecs (particularly within the Oryzoricinae, excluding *M. mergulus*). Studies of the cranial endocasts of marsupial taxa also recover a “elongate” to “rounded” continuum within endocast shape (Weisbecker et al. 2021), another correspondence to conditions amongst the Tenrecomorpha. In contrast, it should be noted that these studies showed little in the way of significant allometric effects. The distinct convergence of phylogenetically distinct semiaquatic taxa and the statistically significant effects of allometry appear, for now, to set this clade of afrosoricids apart.

This is the first study investigating the tenrecomorph sensory apparatus via the use of virtual endocasts derived from high-resolution uCT imaging. Our results provide strong evidence for the influences of phylogeny, allometry, and ecology (as exemplified through ecomorphology and habitat) in the evolution of tenrecomorph taxa. The size and shape of tenrecomorph brains are clearly related, with larger taxa having elongate endocasts and particularly large olfactory bulbs, and smaller taxa having a more “rounded” shape. The clustering of the Oryzoricinae and Potamogalidae suggests the presence of plesiomorphic shapes within each group, which may be related to size in the oryzoricines – removing allometry from the analysis reveals additional variation (particularly with respect to semifossorial taxa) – and to semiaquatic ecology in the case of potamogalids. By contrast, the Tenrecinae and the sole species of Geogalinae are uniquely disparate, occupying widely different regions of the morphospace even under multiple rounds of adjustment for allometry and phylogeny, and lacking ecomorphological clustering with other groups. The distinct strength and significance of allometric and evolutionary signals present in the subfamily groups within Tenrecidae should be kept in mind when analyzing and interpreting the sensory morphology of these clades. Regardless of the root cause of disparity across the species in the clade, this study highlights the exceptional variety of these enigmatic insectivores and presents a foundation for further study of the tenrecomorph sensory system.

Supplementary information The online version contains supplementary material available at <https://doi.org/10.1007/s10914-023-09662-8>.

Acknowledgements Collections made available from the American Museum of Natural History (AMNH) and The Field Museum (FMNH). We would like to thank John Flynn for guidance and assistance throughout, Katie Everson for sharing phylogenetic data, Morgan Hill and Andrew Smith for data management and CT operation assistance, and Neil Duncan, Ellie Hoeger, Marisa Surovy, Sara Ketelson, Bruce Patterson, and Stephanie Smith for access to collections and specimens. Funding in part by National Science Foundation Graduate Research Fellowship Program (NSF GRFP) No. 1447167 and Richard Gilder Graduate School (RGGS) Graduate Fellowship

Author contributions Conceptualization: all authors. CT visualization and morphometric analyses: R.B.S. Providing access to museum collections and equipment: R.D.E.M. Interpretation of anatomical data: all authors. Graphics: R.B.S. Writing: all authors, and approved by all authors.

Funding NSF GRFP No. 1447167, RGGS Graduate Fellowship.

Data availability The data that support the findings of this study are available from the corresponding author, R.B.S., reasonable request.

Code availability All functions listed were run in R ver.4.0.5, with packages *ggPlot* and *Geomorph*. Code is available from the corresponding author upon request.

Declarations

Ethics approval All specimens were loaned and scanned with permissions from their respective collections departments.

Consent to participate N/A

Consent for publication All authors consent to the publication of this study.

Conflicts of interest N/A

References

- Adams DC (2014a) A method for assessing phylogenetic least squares models for shape and other high-dimensional multivariate data: PGLS for high-dimensional data. *Evolution* 68:2675–2688. <https://doi.org/10.1111/evo.12463>
- Adams DC (2014b) A generalized K statistic for estimating phylogenetic signal from shape and other high-dimensional multivariate data. *Syst Biol* 63:685–697. <https://doi.org/10.1093/sysbio/syu030>
- Adams DC, Collyer ML (2018) Phylogenetic ANOVA: Group-clade aggregation, biological challenges, and a refined permutation procedure. *Evolution* 72:1204–1215. <https://doi.org/10.1111/evo.13492>
- Adams DC, Otárola-Castillo E (2013) Geomorph: an R package for the collection and analysis of geometric morphometric shape data. *Methods Ecol Evol* 4:393–399. <https://doi.org/10.1111/2041-210X.12035>
- Ahrens HE (2014) Morphometric study of phylogenetic and ecologic signals in procyonid (Mammalia: Carnivora) endocasts. *Anat Rec* 297:2318–2330. <https://doi.org/10.1002/ar.22996>
- Ali JR, Huber M (2010) Mammalian biodiversity on Madagascar controlled by ocean currents. *Nature* 463:653–656. <https://doi.org/10.1038/nature08706>
- Asher RJ, Hofreiter M, DeBry R (2006) Tenrec phylogeny and the noninvasive extraction of nuclear DNA. *Syst Biol* 55:181–194. <https://doi.org/10.1080/10635150500433649>
- Barton RA, Purvis A, Harvey PH (1995) Evolutionary radiation of visual and olfactory brain systems in primates, bats and insectivores. *Phil Trans R Soc Lond B* 348:381–392. <https://doi.org/10.1098/rstb.1995.0076>
- Bertrand OC, Amador-Mughal F, Lang MM, Silcox MT (2018) Virtual endocasts of fossil Sciuroidea: brain size reduction in the evolution of fossoriality. *Palaeontology* 61:919–948. <https://doi.org/10.1111/pala.12378>
- Bertrand OC, Martin-Flores GS, Silcox MT (2019) Endocranial shape variation in the squirrel-related clade and their fossil relatives using 3D geometric morphometrics: contributions of locomotion and phylogeny to brain shape. *J Zool* 308:197–211. <https://doi.org/10.1111/jzo.12665>
- Buckley M (2013) A molecular phylogeny of *Plesiorycteropus* reassigns the extinct mammalian order ‘Bibymalagasia’ *PLoS ONE* 8(3):e59614
- Butler PM, Hopwood AT (1957) Insectivora and Chiroptera from the Miocene rocks of Kenya Colony. *Foss Mamm Afr* 13:1–35
- Cardini A (2017) Left, right or both? Estimating and improving accuracy of one-side-only geometric morphometric analyses of cranial variation. *J Zool Syst Evol Res* 55:1–10. <https://doi.org/10.1111/jzs.12144>
- Collins CE, Airey DC, Young NA, et al (2010) Neuron densities vary across and within cortical areas in primates. *Proc Natl Acad Sci* 107:15927–15932. <https://doi.org/10.1073/pnas.1010356107>
- Collyer ML, Adams DC (2021) Phylogenetically aligned component analysis. *Methods Ecol Evol* 12:359–372. <https://doi.org/10.1111/2041-210X.13515>
- Dumoncel J, Subsol G, Durrleman S, et al (2021) Are endocasts reliable proxies for brains? A 3D quantitative comparison of the extant human brain and endocast. *J Anat* 238:480–488. <https://doi.org/10.1111/joa.13318>
- Eisenberg JF, Gould E (1969) The tenrecs: a study in mammalian behavior and evolution. *Smithson Contrib Zool* 27:1–137
- Endo H, Koyabu D, Kimura J, et al (2010) A quill vibrating mechanism for a sounding apparatus in the streaked tenrec (*Hemicentetes semispinosus*). *Zoolog Sci* 27:427–432. <https://doi.org/10.2108/zsj.27.427>
- Everson KM, Soarimalala V, Goodman SM, Olson LE (2016) Multiple loci and complete taxonomic sampling resolve the phylogeny and biogeographic history of tenrecs (Mammalia: Tenrecidae) and reveal higher speciation rates in Madagascar’s humid forests. *Syst Biol* 65:890–909. <https://doi.org/10.1093/sysbio/syw034>
- Ferreira JD, Dozo MT, de Moura Bubaduê J, Kerber L (2022) Morphology and postnatal ontogeny of the cranial endocast and paranasal sinuses of capybara (*Hydrochoerus hydrochaeris*), the largest living rodent. *J Morphol* 283:66–90. <https://doi.org/10.1002/jmor.21428>
- Finlay S, Cooper N (2015) Morphological diversity in tenrecs (Afrosoricida, Tenrecidae): comparing tenrec skull diversity to their closest relatives. *PeerJ* 3:e927. <https://doi.org/10.7717/peerj.927>
- Gould E (1965) Evidence for echolocation in the Tenrecidae of Madagascar. *Proc Am Philos Soc* 109:352–360
- Herculano-Houzel S, Catania K, Manger PR, Kaas JH (2015) Mammalian brains are made of these: a dataset of the numbers and densities of neuronal and nonneuronal cells in the brain of Glires, Primates, Scandentia, Eulipotyphlans, Afrotherians and Artiodactyls, and their relationship with body mass. *Brain Behav Evol* 86:145–163. <https://doi.org/10.1159/000437413>
- MacPhee RDE (1986) Environment, extinction, and Holocene vertebrate localities in southern Madagascar. *Natl Geogr Res USA* 2:441–455
- MacPhee RDE (1987) The shrew tenrecs of Madagascar: systematic revision and Holocene distribution of *Microgale* (Tenrecidae, Insectivora). *Am Mus Novit* 2889: 1–45
- MacPhee RDE (1994) Morphology, adaptations, and relationships of *Plesiorycteropus*, and a diagnosis of a new order of eutherian mammals. *Bull Am Mus Nat Hist* 220:1–214
- Materialise Mimics (2020) Materialise Mimics Innovation Suite 22.0. NV Materialise, Leuven, Belgium
- Ni X, Flynn JJ, Wyss AR, Zhang C (2019) Cranial endocast of a stem platyrrhine primate and ancestral brain conditions in anthropoids. *Sci Adv* 5:eaav7913. <https://doi.org/10.1126/sciadv.aav7913>
- Nicoll ME (2003) *Tenrec ecaudatus*, tenrec. In: Goodman SM, Benstead JP (eds) *The Natural History of Madagascar*. University of Chicago Press, Chicago, pp 1283–1287
- Nummela S, Pihlström H, Puolamäki K, et al (2013) Exploring the mammalian sensory space: co-operations and trade-offs among senses. *J Comp Physiol A* 199:1077–1092. <https://doi.org/10.1007/s00359-013-0846-2>
- Olson LE (2013) Tenrecs. *Curr Biol* 23:R5–R8. <https://doi.org/10.1016/j.cub.2012.11.015>
- Olson LE, Goodman SM (2003) Phylogeny and biogeography of tenrecs. In: Goodman SM, Benstead JP (eds) *The Natural History of Madagascar*. University of Chicago Press, pp 1235–1242
- R Core Team (2013) R: A language and environment for statistical computing. R Foundation for Statistical Computing, Vienna, Austria
- Salton JA, Sargis EJ (2008a) Evolutionary morphology of the Tenrecoidea (Mammalia) carpal complex. *Biol J Linn Soc* 93:267–288. <https://doi.org/10.1111/j.1095-8312.2007.00908.x>

- Salton JA, Sargis EJ (2008b) Evolutionary morphology of the Tenrecoidea (Mammalia) forelimb skeleton. In: Sargis EJ, Dagosto M (eds) *Mammalian Evolutionary Morphology*. Springer Netherlands, Dordrecht, pp 51–71
- Salton JA, Sargis EJ (2009) Evolutionary morphology of the Tenrecoidea (Mammalia) hindlimb skeleton. *J Morphol* 270:367–387. <https://doi.org/10.1002/jmor.10697>
- Salton JA, Szalay FS (2004) The tarsal complex of Afro-Malagasy Tenrecoidea: A search for phylogenetically meaningful characters. *J Mamm Evol* 11:73–104. <https://doi.org/10.1023/B:JOMM.0000041190.83655.1d>
- Samonds KE, Godfrey LR, Ali JR, et al (2012) Spatial and temporal arrival patterns of Madagascar's vertebrate fauna explained by distance, ocean currents, and ancestor type. *Proc Natl Acad Sci USA* 1–6. <https://doi.org/10.1073/pnas.1113993109>
- Sánchez-Villagra MR, Asher RJ (2002) Cranio-sensory adaptations in small faunivorous semiaquatic mammals, with special reference to olfaction and the trigeminal system. *Mammalia* 66:93–110
- Sánchez-Villagra MR, Narita Y, Kuratani S (2007) Thoracolumbar vertebral number: the first skeletal synapomorphy for afrotherian mammals. *Systematics and Biodiversity*; Oxford 5:1–7
- Silcox MT, Benham AE, Bloch JI (2010) Endocasts of *Microsyops* (Microsyopidae, Primates) and the evolution of the brain in primitive primates. *J Hum Evol* 58:505–521. <https://doi.org/10.1016/j.jhevol.2010.03.008>
- Stankowich T, Stensrud C (2019) Small but spiny: the evolution of anti-predator defenses in Madagascar tenrecs. *J Mammal* 100:13–20. <https://doi.org/10.1093/jmammal/gyz003>
- Stephan H, Baron G, Frahm HD (1991) *Insectivora: With a Stereotaxic Atlas of the Hedgehog Brain*. Springer-Verlag, New York
- Stephenson PJ, Ganzhorn JU, Rakotoniravony, D (2003) Introduction to the mammals. In: Goodman SM, Benstead JP (eds) *The Natural History of Madagascar*. University of Chicago Press., Chicago and London:, pp 1281–1283
- Stephenson PJ, Racey PA (1993) Reproductive energetics of the Tenrecidae (Mammalia: Insectivora). I. The large-eared tenrec, *Geogale aurita*. *Physiol Zool* 66:643–663
- Sulser RB (2022) An island apart: sensory disparity in phenotype and genotype within the Tenrecomorpha. Dissertation, American Museum of Natural History, New York
- Tabuce R, Asher RJ, Lehmann T (2008) Afrotherian mammals: a review of current data. *Mammalia* 72:2–14. <https://doi.org/10.1515/MAMM.2008.004>
- Thewissen JGM (1985) Cephalic evidence for the affinities of Tubulidentata. *Mammalia* 49:257–284. <https://doi.org/10.1515/mamm.1985.49.2.257>
- Thomas O (1918) On the arrangement of the small Tenrecidae hitherto referred to *Oryzorictes* and *Microgale*. *Ann Mag Nat Hist* 1:302–307. <https://doi.org/10.1080/00222931808562317>
- Watanabe A, Gignac PM, Balanoff AM, et al. (2018) Are endocasts good proxies for brain size and shape in archosaurs throughout ontogeny? *J Anat* 234:291–305 <https://doi.org/10.1111/joa.12918>
- Weisbecker V, Rowe T, Wroe S, et al (2021) Global elongation and high shape flexibility as an evolutionary hypothesis of accommodating mammalian brains into skulls. *Evolution* 75:625–640. <https://doi.org/10.1111/evo.14163>
- Wiley D (2005) *Landmark Editor 3.6*. Institute for Data Analysis and Visualization, University of California, Davis
- Zelditch ML, Swiderski DL, Sheets HD (2012) *Geometric Morphometrics for Biologists: A Primer*. Academic Press, Boston, MA

Springer Nature or its licensor (e.g. a society or other partner) holds exclusive rights to this article under a publishing agreement with the author(s) or other rightsholder(s); author self-archiving of the accepted manuscript version of this article is solely governed by the terms of such publishing agreement and applicable law.